Int. J. Heat Mass Transfer. Vol. 17. pp. 1003 1018. Pergamon Press 1974. Printed in Great Britain

TURBULENT HEAT TRANSFER IN A CIRCULAR TUBE WITH CIRCUMFERENTIALLY VARYING THERMAL BOUNDARY CONDITIONS*

D. GÄRTNER, K. JOHANNSEN and H. RAMM
Heat Transfer Group, Institute of Nuclear Engineering, Technical University of Berlin, Marchstr. 18, Berlin 10, Germany

(Received 12 June 1973)

Abstract—An analysis has been carried out to determine the heat-transfer characteristics for turbulent flow in circular tube with circumferentially varying boundary conditions of first and second kind. Fully developed flow and heat transfer is considered. Contrary to prior investigations of this problem, anisotropy of turbulent energy transport has been taken into account employing theoretical results for eddy diffusivity in the various directions from an analysis of Ramm and Johannsen which are shown to be in satisfactory agreement with recent experimental data. Results for heat transfer at both constant and varying boundary conditions are presented over a wide range of Reynolds number ($10^4 \leqslant Re \leqslant 10^6$) and Prandtl number ($0 \leqslant Pr \leqslant 100$) and compared to empirical data.

NOMENCLATURE

a, b, Fourier coefficients;
C_p, specific heat at constant pressure;
E, diffusivity function, $(1+\varepsilon_H/\alpha)$;
F, dimensionless wall heat flux variation about the mean;
f, Fanning friction factor;
g, dimensionless temperature difference function;
G, wall temperature function;
k, thermal conductivity;
n, harmonic;
Nu, Nusselt number;
Pr, Prandtl number;
q, heat flux;
r, radial coordinate;
r_0, tube radius;
R, radial temperature function;
Re, Reynolds number;
t, dimensionless fully-developed fluid temperature; above mixed mean, $[T(\rho,\varphi)-T_m].k/q_0.r_0$;
T, temperature;
u, velocity;
U, dimensionless velocity, u/u_m;
y^+, dimensionless distance, $\hat{\rho}.\sqrt{(\tau_w/\rho^*)}/\nu$.

Greek symbols
α, thermal diffusivity, $k/\rho^*.C_p$;
ε, eddy diffusivity;
ν, kinematic viscosity;
ρ, dimensionless radial coordinate, r/r_0;
$\hat{\rho}$, dimensionless distance from wall, $(1-\rho)$;
ρ^*, fluid density;
τ, shear stress;
φ, angular coordinate.

Subscripts and superscripts
anis, anisotropic;
0, average;
D, mass;
D–B, Dittus–Boelter, cf. equation (30);
H, heat;
is, isotropic;
m, mixed mean;
mc, molecular conduction;
M, momentum;
n, harmonic;
r, radial direction;
s, starting point index;
w, wall;
φ, circumferential direction;
∞, asymptotic (fully-developed);
$*$, prescribed wall temperature.

INTRODUCTION

ALTHOUGH the circular tube is the probably most common geometry used to study the basic problems of heat transfer to turbulent internal flows, only a very limited number of investigations has dealt thus far with the effect of circumferentially non-uniform thermal boundary conditions. As far as theoretical work is concerned, this situation may be due to the unavailability of pertinent experimental or theoretical data on

*Dedicated to Professor h. Professor Dr. sc. techn. Romano Gregorig on the occasion of his 65th birthday.

the thermal diffusivity in the circumferential direction. Prior analyses of turbulent heat transfer in a tube with circumferentially varying boundary conditions as of Reynolds [1] as well as of Sparrow and Lin [2] have thus been based on the key assumption that the diffusivities of heat in the radial and tangential directions are identical. Black and Sparrow [3, 4] who performed the only experimental investigation with a non-uniformly heated circular tube the present authors are aware of, also extended the Sparrow–Lin analysis to accommodate a (constant) ratio of tangential to radial eddy diffusivity different from unity. Results for the temperature fields obtained on this basis have been compared with the measured temperature profiles. From this comparison Black and Sparrow concluded that the eddy diffusivity ratio, $\varepsilon_{H\varphi}/\varepsilon_{Hr}$, may be well in excess of unity in the neighbourhood of the wall, where turbulent eddies have greater freedom for tangential motion than for radial motion, but is essentially unity at all other points in the flow. This conception of the transport process has been confirmed by results of a combined theoretical and experimental approach of Bobkov *et al.* [5] and of an analysis of Ramm and Johannsen [6] to evaluate diffusivities. Very recently, experimental results for heat and mass transfer by Quarmby and Quirk [26] have strongly supported these previous findings.

In this paper, thermal eddy diffusivity distributions which are different in both directions as well as the velocity profiles of the Ramm–Johannsen analysis are used to resolve the problem of turbulent heat transfer in a circular tube with circumferentially varying thermal boundary conditions. The results of the analysis show the effects of Reynolds number and Prandtl number as well as of anisotropic turbulent thermal diffusivity on heat transfer. The agreement with the only available experimental results, those of Black and Sparrow [3, 4], is found to be satisfactory. Although restricted to a particular simple case, the present analysis provides some general insight into the nature and magnitude of the effects of circumferentially nonuniform boundary conditions on turbulent heat transfer.

ANALYSIS

We consider a turbulent tube flow with fully established velocity and temperature fields in which there is a uniform heat-transfer rate per unit length but in which either the wall temperature or the wall heat flux may vary arbitrarily around the circumference. Neglecting viscous dissipation and assuming constant fluid properties, the governing differential equation for the fully developed fluid temperature may be written in dimensionless form as

$$L(t) = 2U(\rho), \tag{1}$$

where we denoted for brevity

$$L = \frac{1}{\rho}\frac{\partial}{\partial\rho}\left[\rho\,.\,E_r\,.\,\frac{\partial}{\partial\rho}\right] + \frac{1}{\rho^2}\,.\,\frac{\partial}{\partial\varphi}\left[E_\varphi\,.\,\frac{\partial}{\partial\varphi}\right]. \tag{2}$$

The thermal transport function E in the various directions is taken to be a function of the radial coordinate ρ only, since it is assumed that the turbulent energy transport is set up by the axisymmetric flow field and thus independent of the thermal boundary conditions. Though one might expect that the boundary conditions have an influence, no evidence of this effect can be drawn from the pertinent experimental data, since probably any differences which may have occurred due to different boundary conditions are concealed in their scatter. Thus the assumption of taking $E = f(\rho)$ seemed appropriate in view of present knowledge.

The solution of equation (1) must be such that the mixed mean of the dimensionless temperature difference $t(\rho, \varphi)$ is zero, i.e.

$$\int_0^1 \int_0^{2\pi} t(\rho, \varphi)\,.\,U(\rho)\,.\,\rho\,.\,\mathrm{d}\varphi\,\mathrm{d}\rho = 0. \tag{3}$$

Case 1: *Prescribed wall heat flux*

If the wall heat flux is prescribed to vary in an arbitrary manner around the circumference as given by $F(\varphi)$, the associated boundary condition may be formulated as

$$\left(\frac{\partial t}{\partial\rho}\right)_{\rho=1} = 1 + F(\varphi). \tag{4}$$

We restrict ourselves to cases where the heat flux variation $F(\varphi)$ may be expressed in terms of Fourier series and put

$$F(\varphi) = \sum_{n=1}^{\infty} F_n(\varphi), \tag{5}$$

where

$$F_n(\varphi) = a_n\,.\cos n\varphi + b_n\,.\sin n\varphi, \tag{6}$$

and

$$\int_0^{2\pi} F(\varphi)\,\mathrm{d}\varphi = 0. \tag{7}$$

Taking cognizance of equation (4) we choose to write the temperature difference $t(\rho, \varphi)$ as the following sum,

$$t(\rho, \varphi) = g_0(\rho) + g(\rho, \varphi), \tag{8}$$

where $g_0(\rho)$ is seen to be the temperature difference above mixed mean associated with the average heat flux q_0, and $g(\rho, \varphi)$ is the temperature difference above $g_0(1)$ which takes care of the heat flux variation, g_0 is the solution of the inhomogeneous ordinary differential equation

$$L(g_0) = 2\,.\,U(\rho) \tag{9a}$$

subject to boundary conditions

$$g_0(0) = 0 \quad \text{and} \quad g_0'(1) = 1. \tag{9b}$$

The appropriate condition (3) on equation (9a) is

$$\int_0^1 g_0(\rho) \,.\, U(\rho) \,.\, \rho \,.\, \mathrm{d}\rho = 0. \tag{9c}$$

To find the governing equation for $g(\rho, \varphi)$ we introduce equation (8) into the energy equation (1). Taking account of the fact that g_0 satisfies equations (9), it follows that $g(\rho, \varphi)$ must obey

$$L(g) = 0. \tag{10}$$

It is interesting to note that the velocity term does not appear in equation (10), and thus g is independent of the velocity field. We seek a solution for g in the form of a product

$$g(\rho, \varphi) = R(\rho) \,.\, F(\varphi). \tag{11}$$

The function $F(\varphi)$ is defined by equations (5)–(7) and the solution for g may then be obtained in the form

$$\begin{aligned} g(\rho, \varphi) &= \sum_{n=1}^{\infty} R_n(\rho) \,.\, F_n(\varphi) \\ &= \sum_{n=1}^{\infty} R_n(\rho) \,.\, (a_n \cos n\varphi + b_n \sin n\varphi). \end{aligned} \tag{12}$$

The radial temperature functions $R_n(\rho)$ must satisfy

$$\frac{\mathrm{d}}{\mathrm{d}\rho}\left[E_r(\rho) \,.\, \rho \,.\, \frac{\mathrm{d}R_n}{\mathrm{d}\rho}\right] - n^2 \frac{E_\varphi(\rho)}{\rho} R_n = 0 \tag{13a}$$

with boundary conditions

$$R_n(0) = 0 \quad \text{and} \quad R_n'(1) = 1. \tag{13b}$$

The boundary value problems (9) and (13) have been solved applying a modified fifth order Runge–Kutta integration procedure. Since equation (13a) has a singularity at $\rho = 0$ the integration was started near $\rho = 0$ and carried then to the wall. To start the Runge–Kutta procedure we made use of the laminar solution at the starting point ρ_s near the tube center [1]:

$$R_n(\rho_s) = \rho_s^n / n$$

and

$$R_n'(\rho_s) = \rho_s^{n-1}.$$

Because of the homogeneity of equation (13a), the radial temperature functions computed from the integration may be multiplied by any constant, and could therefore be normalized by

$$c = 1/R_n'(1)$$

or, if the wall temperature around the periphery is prescribed (Case 2), by

$$c^* = 1/R_n^*(1)$$

to match the boundary conditions (13b) or (13c), respectively.

The computations were performed using sixty to seventy increments (the more the higher the Reynolds number) which have been distributed in exactly the same manner as has been proved favourable in the computational procedure for determining the velocity and thermal eddy diffusivity profiles. There the grid spacing was chosen such that the velocity differences between two grid points were approximately the same over the entire radius resulting in a very dense distribution in the wall near region where large velocity gradients exist.

To check the convergence of solutions obtained by this integration procedure, first the laminar case has been treated where analytical solutions are available [1]. At least, five-figure agreement was found for the first six harmonics.

Then the velocity and eddy diffusivity distributions of the Ramm–Johannsen analysis as of present yet unpublished status of development were introduced to calculate the turbulent temperature functions for the first harmonics. Using ten times as many increments it was found that solutions changed less than 0·1 per cent even at the highest Reynolds and Prandtl numbers for which results are reported herein. Since largest error occurs under these conditions, accuracy of all results for turbulent heat transfer is to better than 0·1 per cent.

Having the solutions at hand, we denote the boundary values of the radial temperature functions

$$G_0 = g_0(1) \tag{14}$$

and

$$G_n = R_n(1), \quad n = 1, 2, \ldots, \tag{15}$$

which depend parametrically on Reynolds and Prandtl numbers. The dimensionless circumferential wall temperature above mixed mean corresponding to an arbitrarily prescribed heat flux $F(\varphi)$ may then be written as

$$t(1, \varphi) = G_0 + \sum_{n=1}^{\infty} G_n \,.\, (a_n \cos n\varphi + b_n \sin n\varphi). \tag{16}$$

The local asymptotic Nusselt number is therefore

$$Nu_\infty(\varphi) = \frac{2 \,.\, q(\varphi)/q_0}{G_0 + \sum_{n=1}^{\infty} G_n \,.\, F_n(\varphi)} \tag{17}$$

while the Nusselt number for uniform heat flux is simply

$$Nu_{\infty 0} = 2/G_0. \tag{18}$$

Case 2: Prescribed wall temperature

If the wall temperature is prescribed to vary arbitrarily around the circumference, it may now be formulated according to previous analysis as

$$t(1,\varphi) = g_0(1)+g^*(1,\varphi) = G_0+\sum_{n=1}^{\infty} R_n^*(1).F_n^*(\varphi) \tag{19}$$

where

$$F_n^*(\varphi) = a_n^*\cos n\varphi + b_n^*\sin n\varphi. \tag{6a}$$

The relations (5) and (7) hold for F_n^* as well.

The radial temperature functions $R_n^*(\rho)$ appearing in the formulation of the local fluid temperature corresponding to a prescribed wall temperature,

$$t(\rho,\varphi) = g_0(\rho)+\sum_{n=1}^{\infty} R_n^*(\rho).F_n^*(\varphi), \tag{20}$$

must again satisfy equation (13a) but with the boundary conditions

$$R_n^*(0) = 0 \quad \text{and} \quad R_n^*(1) = 1. \tag{13c}$$

The numerical solution of equation (13a) with (13c) may be performed as described before.

The local heat flux around the periphery of the tube, $q(\varphi)$ is now obtained differentiating the temperature as of equation (20) with respect to ρ at the tube wall. Normalizing $q(\varphi)$ by the average wall heat flux,

$$q_0 = \left(\frac{dg_0}{d\rho}\right)_{\rho=1}, \tag{21}$$

one obtains

$$\frac{q(\varphi)}{q_0} = 1+\sum_{n=1}^{\infty}\left(\frac{dR_n^*}{d\rho}\right)_{\rho=1}.F_n^*(\varphi). \tag{22}$$

At the tube wall ($\rho = 1$), the solutions for both cases of circumferentially varying boundary conditions are closely related to each other since

$$\left(\frac{dR_n^*}{d\rho}\right)_{\rho=1} = \frac{1}{R_n(1)}, \tag{23}$$

and

$$F_n^* = F_n.R_n(1). \tag{24}$$

Thus using the relation (23), the wall heat flux may be immediately obtained from equation (22) if Case 1 has been solved previously. Vice versa, if the heat flux is prescribed and $(dR_n^*/d\rho)_{\rho=1}$ is available having solved equation (13a) for R_n^* with boundary conditions (13c), the circumferential wall temperature variation may be found from equation (16) applying equations (15) and (23). In practice, the first way is preferred because the radial temperature functions as obtained from equation (13a) are more accurate than their derivatives.

TURBULENT THERMAL DIFFUSIVITY

For solving the differential equations (9) and (13) information on turbulent properties of the flow is needed. The temperature difference above mixed mean, $g_0(\rho)$, associated with the average heat flux q_0 may be evaluated as the turbulent velocity profile $U(\rho)$ and the distribution of thermal diffusivity in the radial direction, $\varepsilon_{Hr}(\rho)$, are known. In the radial temperature functions $R_n(\rho)$ only the thermal eddy diffusivity but for both the radial and circumferential direction is involved.

All this input information has been taken directly from the analysis of Ramm and Johannsen to predict momentum and heat transfer in fully developed turbulent channel flow [6, 7]. This theoretical approach falls into the category of phenomenological turbulence-model approaches or may be considered as a "zero-equation statistical turbulence model". It is based on the principal ideas of Buleev's model of turbulent transfer in three-dimensional fluid flow [8, 9] which permits the determination of all the components of the turbulent shear stress tensor as well as the turbulent heat fluxes *independently* of each other. However, application of Buleev's model to different channel geometries for predicting fluid flow and heat transfer has shown that results obtained become very unsatisfactory in view of both physical reasoning and experimental evidence as limits of geometric parameters are approached (i.e. for example for annular flow, if radius ratio approaches zero). This wrong behavior of the solutions which is most obvious if the turbulent transport properties are considered, can only be attributed to severe deficiencies of the model. Thus Ramm and Johannsen carefully reviewed the assumptions of Buleev's model as well as the derivation of the calculational method which resulted in essential improvements and extensions of the original approach which are described in some detail in [37]. The improved method has been applied to predict turbulent flow and heat transfer in smooth channels of uniform (circular) and non-uniform cross section [6, 7, 13, 28, 37].

Preliminary results obtained for velocity profiles and eddy diffusivities in plane, circular, and concentric annular ducts showed very satisfactory agreement with the available experimental data [6]. In the present paper, however, results of the latest state of development of the method have been used. This is essentially identical to that described in [7], however, the effect of dissipation, which previously has been assumed constant, has now been introduced to depend strongly both on position in the flow channel and Reynolds number in accordance with empirical evidence. This change has been proved rather important mainly in view of extending the applicability of the method to medium and high Prandtl number heat transfer.

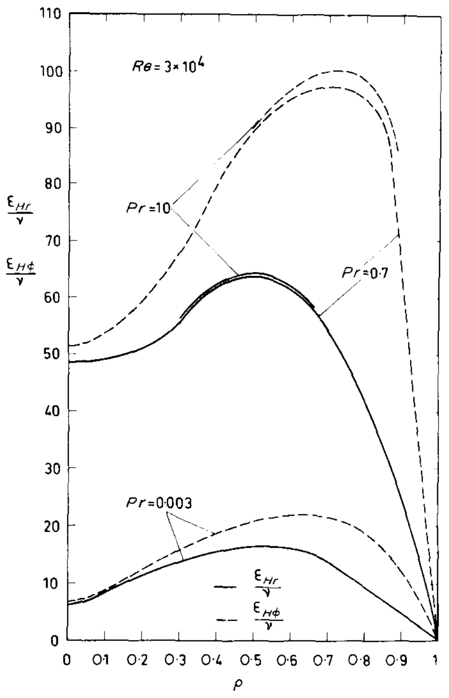

FIG. 1. Typical distributions of turbulent diffusivities of heat in the radial and circumferential directions for turbulent flow in a circular tube.

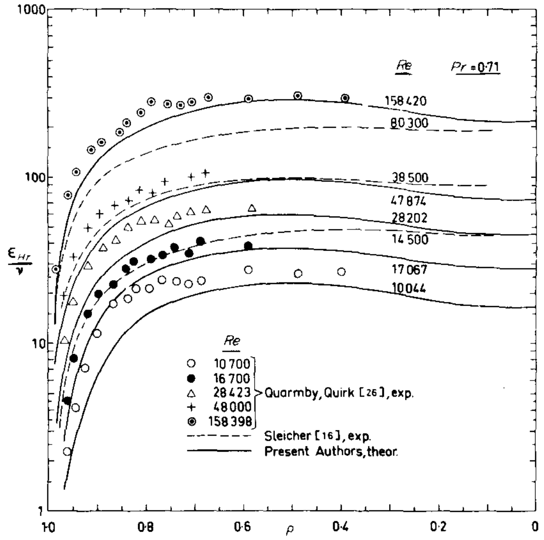

FIG. 2. Radial eddy diffusivity of heat vs relative tube radius.

In the context of the present paper, results for the eddy diffusivity of heat are of main interest. As experimental data indicate, ε_H has been found to be a function of the Reynolds number, the Prandtl number, and the position as well as the direction in the channel. Typical distributions of ε_H in both the radial and circumferential direction are shown in Fig. 1 for a Reynolds number of 30 000. The most interesting finding is that the diffusivity in the tangential direction, $\varepsilon_{H\varphi}$, varies appreciably almost across the entire flow section. Only at the center of the tube ε_H is independent of direction for reason of symmetry.†

Predictions for ε_{Hr} are compared to recent measurements of Quarmby and Quirk [26] and previous experimental results of Sleicher [16] in Fig. 2. It can be seen that the agreement is satisfactory.

The anisotropy of eddy transport is a strong function of the position in the channel. The predicted ratio $\varepsilon_{H\varphi}/\varepsilon_{Hr}$, as shown in Fig. 3 versus wall distance for various Reynolds numbers, exhibits a sharp maximum in the region close to the wall. It decreases to a value of unity as the center of the tube is approached.† This principal behavior has also been suggested by turbulence measurements (Laufer [10], Lawn and Elliott [11] and others) and the attempts of Black and Sparrow [3, 4] and Quarmby [12] who tried different

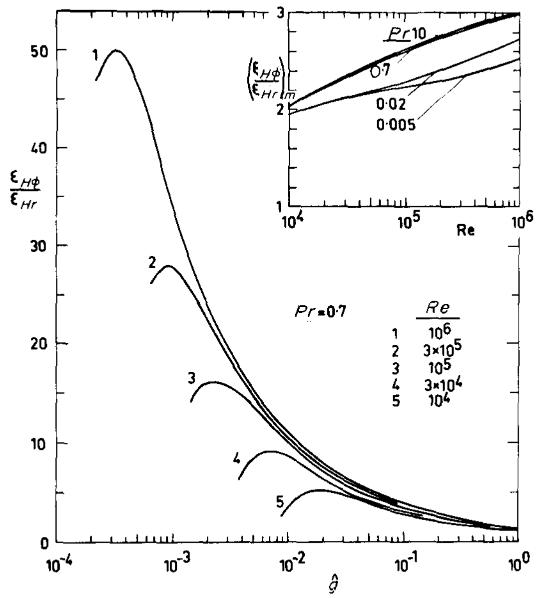

FIG. 3. Ratio of eddy diffusivity for heat in the tangential direction to that in radial direction vs relative wall distance.

†Since in the present calculational method the turbulence properties at the center position of the tube are determined by integration procedures over the surrounding neighbourhood the ratio does not approach exactly the expected value of 1·0 at point $\rho = 0$ but a slightly greater one in the order of magnitude of 1·03 to 1·05.

assumptions on the radial variation of the eddy diffusivity ratio to bring theory and experiment into agreement. The only direct results which the present predictions may be compared with seem to be those published by Bobkov *et al.* [5] and, very recently, by Quarmby and Quirk [26].

The approach by Bobkov *et al.* is a combined theoretical and experimental one, because it involves an experimental investigation of the statistical characteristics of temperature fluctuations and a subsequent theoretical analysis involving the theory of homogeneous turbulent diffusion for limited regions of the flow. Their $\varepsilon_{H\varphi}/\varepsilon_{Hr}$-results for the circular tube are presented in graphical form as data points which also have been approximated by the following equation:

$$\frac{\varepsilon_{H\varphi}}{\varepsilon_{Hr}} = 1 + \frac{0{\cdot}2}{1{\cdot}02 - \rho}. \tag{25}$$

It may be noted that both presentations are independent of Reynolds number as well as Prandtl number, though the authors state a weak dependence of the diffusivity ratio on Re. The present predictions have been compared with those results in [27], and excellent agreement has been found in the ranges of $\rho \leqslant 0{\cdot}95$ and $Re < 10^5$.

The experimental results for heat transfer of Quarmby and Quirk [26] were obtained using an electrically heated wall patch source in a plain tube under conditions of fully developed turbulent flow. They are compared together with data for mass transfer reported by the same authors to present predictions in Fig. 4. In view of the scatter of the data, the agreement is very satisfactory. As in Fig. 3, predictions indicate an increase of the diffusivity ratio with Reynolds number as far as the wall near region is concerned. This effect, however, seems to fall well within the limits of experimental uncertainty and is thus not evident in the measurements.

Considering the average values of the $\varepsilon_{H\varphi}/\varepsilon_{Hr}$-ratio as effected by variations in Reynolds number and Prandtl number (Fig. 3), it is seen that anisotropy increases slightly with increasing both Re and Pr. The effect of Prandtl number changes is less important and only noticeable at low Prandtl numbers.

Typical distributions of the diffusivity function E in both directions as used in the calculations are shown in Fig. 5. It may be noted that the local variations of E increase and become the more concentrated in the wall near region the higher both Re and Pr.

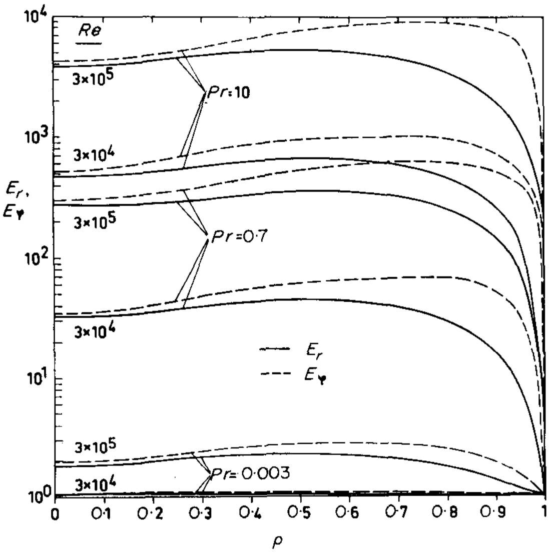

FIG. 5. Diffusivity function E in the radial and tangential directions vs relative tube radius for different Reynolds numbers and Prandtl numbers.

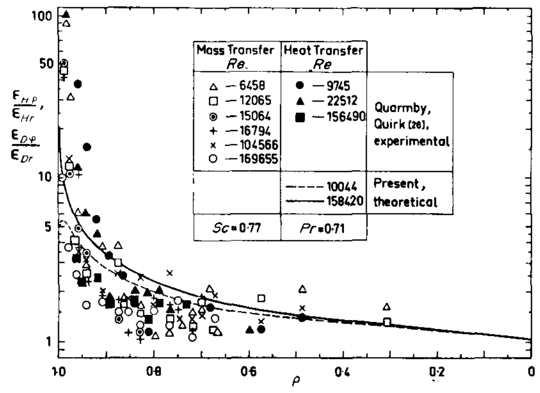

FIG. 4. Ratio of mass and heat eddy diffusivities in the tangential directions to that in radial direction vs relative radius.

It may be pointed out that in the previous analyses of the effect of circumferentially varying boundary conditions [1–4, 14] not only the anisotropy of E has been neglected but also a more simplified approach for its evaluation has been applied. E_r has been rewritten as

$$E_r = 1 + \frac{\varepsilon_{Mr}}{\nu}\,\frac{\varepsilon_{Hr}}{\varepsilon_{Mr}}.\,Pr, \tag{26}$$

and separate assumptions for the eddy diffusivity of momentum, ε_{Mr}/ν, and the diffusivity ratio, $\varepsilon_{Hr}/\varepsilon_{Mr}$, have been made. In principle, there is obviously nothing wrong with this procedure as long as $\varepsilon_{Hr}/\varepsilon_{Mr}$ is also taken as a function of position and is consistent with the relation for ε_{Mr}/ν. However, in these analyses

$\varepsilon_{Hr}/\varepsilon_{Mr}$ has throughout been represented by the ratio of the local averages and thus taken constant. Sparrow and Lin [2] as well as Black and Sparrow [3, 4] assumed the ratio to be unity for $Pr = 0{\cdot}7$ and 10, while Reynolds [1], and recently, Rapier [14] used the Jenkins' correlation [15] multiplied by a factor of 1·15 for $Pr \leqslant 0{\cdot}7$ and a constant value of 1·15 for $Pr \geqslant 3$.

Figure 6 compares the local distribution of $\varepsilon_{Hr}/\varepsilon_{Mr}$ as obtained from the Ramm–Johannsen analysis with experimental results of Sleicher [16], Kjellström [17] and Quarmby and Quirk [26] for air. Both theory and experimental data indicate that the eddy diffusivity ratio, besides being dependent on Reynolds number and Prandtl number, is also a function of the position in the channel. The variation of $\varepsilon_{Hr}/\varepsilon_{Mr}$ is most pronounced in the wall near region and extends more to the center as Reynolds and Prandtl numbers decrease. It seems worth mentioning that for $Pr \leqslant 0{\cdot}5$ the ratio increases near the wall with wall distance while the opposite is true for higher Prandtl numbers. This predicted behavior gains some support from experimental results. However, especially in the low Prandtl number range, no clear impression regarding the true behavior emerges due to the large scatter of data. The general agreement with Sleicher's and Kjellström's results for air seems to be good in view of the experimental uncertainties.

The average values of the diffusivity ratio in the radial direction as used in the analyses of Reynolds [1] and

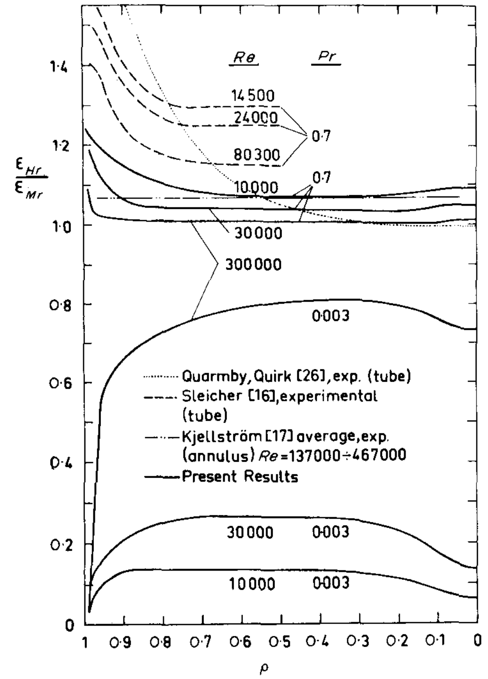

FIG. 6. Ratio of radial heat diffusivity to that of momentum vs relative radius.

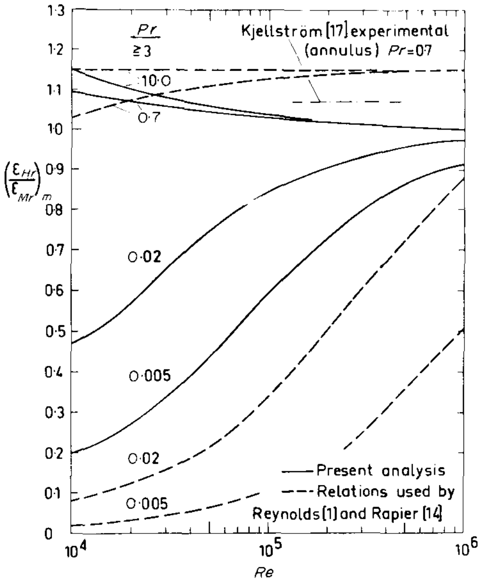

FIG. 7. Average ratio of radial heat diffusivity to that of momentum vs Reynolds number.

Rapier [14] are compared to present predictions in Fig. 7. For $Pr = 0{\cdot}7$, the agreement between both predictions as well as with the experimental data of Kjellström is not bad, however, the effect of Reynolds number in Jenkins' correlation is just vice versa to that observed in the experimental data (Fig. 6) and present theoretical results. Though the majority of data seems to indicate that, at $Pr = 0{\cdot}7$, the diffusivity ratio decreases slightly with increasing Reynolds number [17], it can be stated that the situation is far from being clear and also other theories exist which agree with the trends of Jenkins' prediction (e.g. Tyldesley and Silver [18]). In the low Prandtl number range, remarkable discrepencies between results of present theory and the Reynolds/Rapier assumption exist. Since, for a Prandtl number of 0·007, the present predictions are in excellent agreement with recent experimental data [19, 20, 21] as demonstrated in [6, 28, 37], it is felt that Jenkins' relation can be considered to be incorrect at Prandtl numbers less than say 0·1.

DISCUSSION AND COMPARISON OF RESULTS

Constant wall heat flux

To check the validity of present results, the asymptotic Nusselt number, $Nu_{\infty 0}$, for a uniform axial heat flux distribution as calculated from equation (18) has been compared with empirically well-established correlations and single experimental results for fully developed turbulent heat transfer in a circular tube (Figs. 11–13).

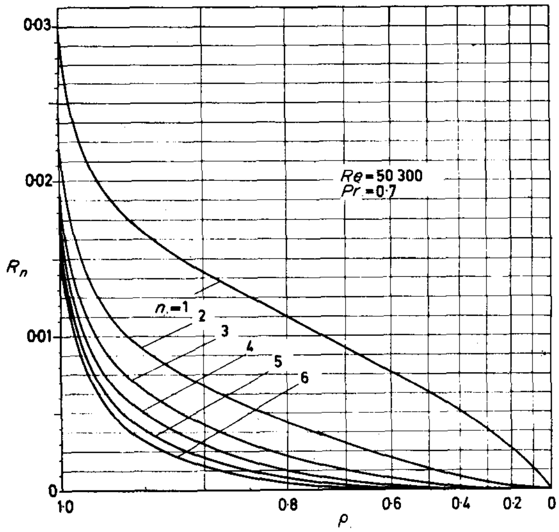

FIG. 8. Typical radial temperature functions for the case of prescribed wall heat flux.

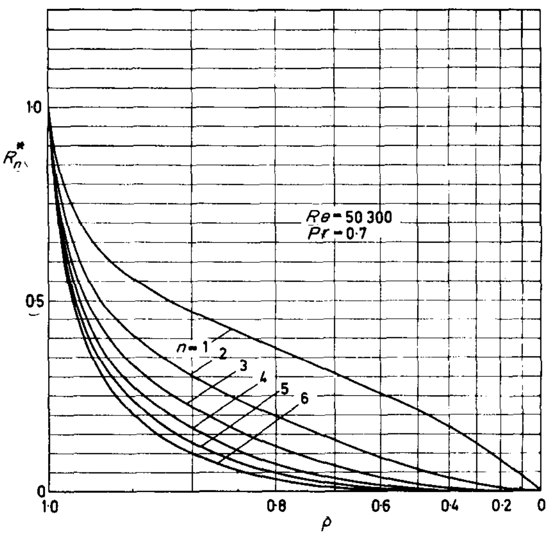

FIG. 9. Typical radial temperature functions for the case of prescribed wall temperature.

In Fig. 11, emphasis is devoted to the low Prandtl number range. Subbotin *et al.* [22] correlated experimental data on measured turbulent heat-transfer coefficients with flow of various fluids and found the following formula:

$$Nu_{\infty 0} = (Nu_{\infty 0})_{mc} + 0·0155 \times Re^{0·82} \times Pr^n, \quad (27)$$

where

$$(Nu_{\infty 0})_{mc} = 7·24 - 9·5/\log Re,$$

and

$$n = 0·58 - 0·18 \,.\, \tanh(0·8 \times \log Pr).$$

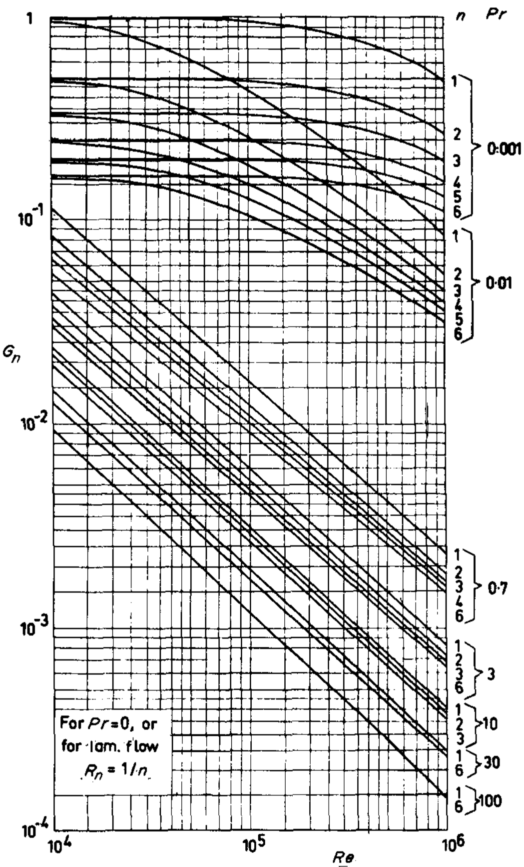

FIG. 10. Radial temperature functions at the wall for the case of prescribed wall heat flux as a function of Reynolds number and Prandtl number.

Equation (27) is claimed to represent a large number of data in the ranges of $0 < Pr \leqslant 5$ and $10^4 \leqslant Re \leqslant 5 \times 10^5$ with a scatter of ± 12 per cent, if correlated in coordinates $Nu_{\infty 0}$ vs $Re^{0·82} Pr^n$. It takes no account of the temperature dependence of the fluids physical properties. For $Pr \leqslant 0·7$, the agreement of relation (27) with present results appears to be excellent except at very low Prandtl and Reynolds number, where empirical results still are somewhat in doubt and contradictory. However, the value predicted for the limiting Nusselt number ($Pr \to 0$) at $Re = 10^4$ of approximately 6 lies well between other empirical and theoretical correlations which indicate values from about 5 to 7. For $Pr \geqslant 0·7$, comparison is also made to a simple relation of the form

$$Nu_{\infty 0} = C\, Re^m, \quad (28)$$

where however, the parameters C and m are taken as function of Prandtl number [23]. For isothermal conditions, numerical values for C and m have been

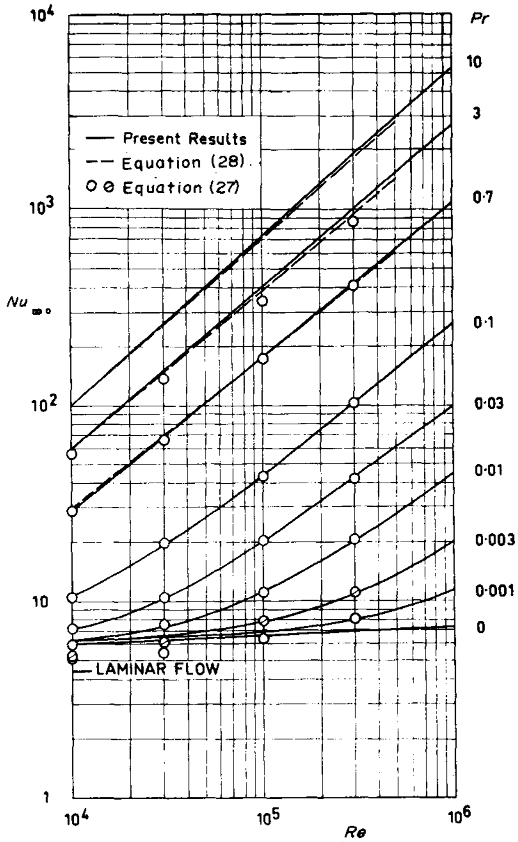

FIG. 11. Results and comparisons for fully-developed heat transfer at constant wall heat flux, PR $\leqslant$ 10.

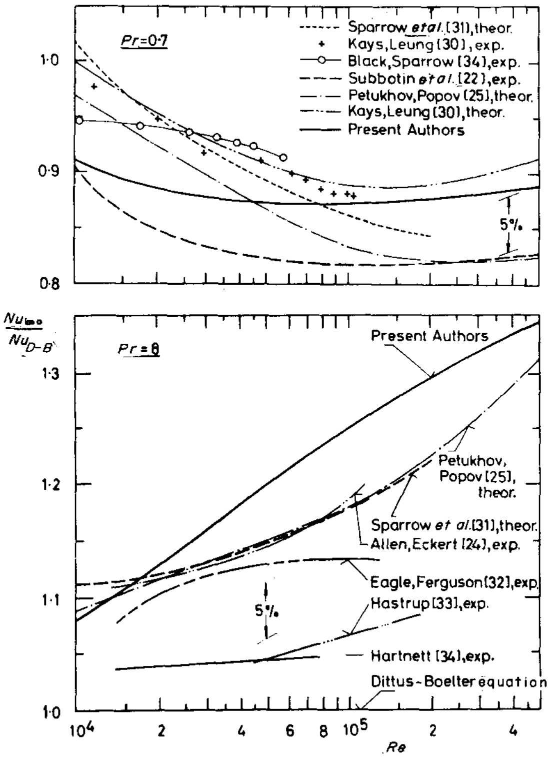

FIG. 12. Results and comparisons for fully-developed heat transfer at constant wall heat flux, $Pr = 0{\cdot}7$ and 8.

determined by Hufschmidt *et al.* [23] for $0{\cdot}7 \leqslant Pr \leqslant 10$ and $10^4 \leqslant Re \leqslant 5 \times 10^5$ adjusting graphically equation (28) to the theoretical relation of Petukhov and Popov [25],

$$Nu_{\infty 0} = \frac{(f/2) \times Re \times Pr}{1{\cdot}07 + 12{\cdot}7 \times \sqrt{[(f/2) \times (Pr^{2/3} - 1)]}}, \quad (29)$$

which they found to agree best with both their own measurements and those of Allen and Eckert [24]. Very recently, Webb [29] also claimed that relation (29) provides a very good correlation of existing data for $0{\cdot}7 < Pr < 50$ and agrees with the smoothed results of four investigators within ± 15 per cent. Thus assigning to relation (29) and its simplified form (28) a sound degree of reliability, present analysis seems to slightly overpredict Nusselt number at $Pr = 3$ and 10 in the high Reynolds number range.

A more detailed comparison of present results with appropriate analytical and empirically based predictions for the range of $0{\cdot}7 \leqslant Pr \leqslant 75$ is made in Figs. 12 and 13. The ordinates are normalized by Nusselt numbers computed from the Dittus–Boelter correlation:

$$Nu_{D\ B} = 0{\cdot}023\, Re^{0{\cdot}8}\, Pr^{0{\cdot}4}. \quad (30)$$

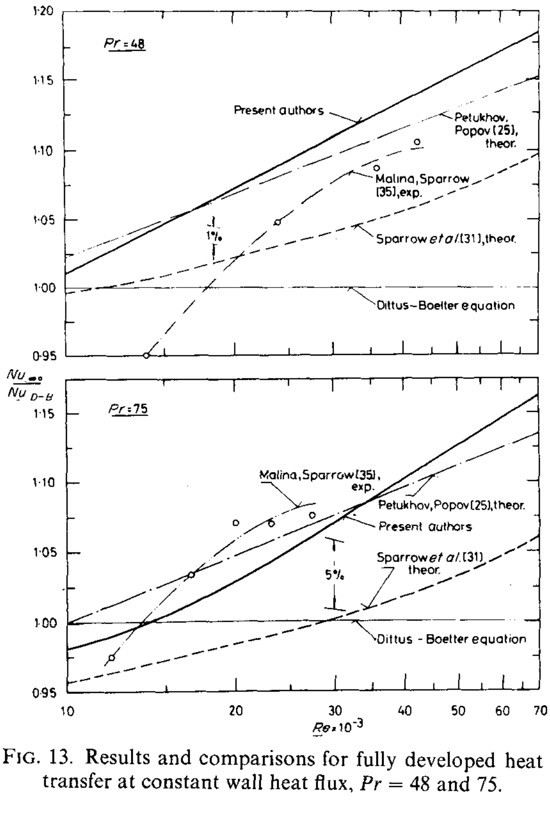

FIG. 13. Results and comparisons for fully developed heat transfer at constant wall heat flux, $Pr = 48$ and 75.

Inspection of Figs. 12 and 13 reveals that, at all Prandtl numbers which a comparison is made for the deviations between present theory and experimental results do not exceed 10 per cent and are generally much less.† Best agreement is obtained at the high Prandtl numbers (Fig. 13); neglecting the low Reynolds number test of Malina and Sparrow [35] at $Pr = 48$ (upper graph of Fig. 13), deviations between both the empirical results [35] and the realtion of Petukhov and Popov [25] are always less than 4 per cent for $10^4 \leqslant Re \leqslant 7 \times 10^4$. All results including those from present authors also indicate, that for $Pr = 8$ the dependence of the Nusselt number upon Reynolds number exceeds the power of 0·8 and thus the Dittus–Boelter equation (30) tends to give the more conservative results the higher the Reynolds number. This finding has also been cited by previous investigators [23, 35].

The foregoing comparisons are felt to demonstrate to a sufficient extent that the theoretical method of Ramm and Johannsen may be used over a wide range of Prandtl number ($0 \leqslant Pr \leqslant 100$) to predict turbulent heat transfer in a circular tube with very satisfactory accuracy.

Varying boundary conditions

The properties of the heat-transfer solutions obtained for a circumferentially varying heat flux probably may be discussed most conveniently in terms of the ratio G_n/G_0 $(n \geqslant 1)$, which in a sense is a measure of the relative importance of the higher harmonics and the average. Consider, for instance, the case of a tube heated with a cosinusoidally varying heat flux distribution around the periphery of amplitude a_n

$$\frac{q(\varphi)}{q_0} = 1 + a_n . \cos n\varphi. \tag{31}$$

Using equation (16), the dimensionless local wall temperature difference is found to be

$$\begin{aligned} t(1, \varphi) &= G_0 + a_n . G_n . \cos n\varphi \\ &= G_0 . \left(1 + a_n . \frac{G_n}{G_0} . \cos n\varphi\right). \end{aligned} \tag{32}$$

If the average Nusselt number is used to estimate the circumferential wall temperature variation due to the varying heat flux as of equation (31), it immediately follows from equation (32) that the amplitude of the temperature variation is identical to that of the heat flux. Thus, for each harmonic of the heat flux variation, the ratio G_n/G_0 describes the increase or decrease of the wall temperature amplitude relative to that one would obtain if the average heat-transfer coefficient is employed.

†The results of Hartnett's experiments for $Pr = 8$ have not been taken into account, for they were not extrapolated to the constant-property condition.

In Figs. 14–16, the ratio G_n/G_0 has been plotted for the first, third and sixth harmonic, respectively. The figures exhibit quite a number of interesting features. It should first be noted that the ratio of G_n/G_0 for pure molecular conduction ($Pr = 0$) proves to become the limiting value as the contribution of turbulent diffusion to energy transfer decreases with decreasing Reynolds and Prandtl numbers. The molecular condition curve also clearly tends to approach the corresponding slug flow ratio as, with $Re \to \infty$, the turbulent velocity profile becomes flatter and flatter. It has to be pointed out, however, that the curves for $Pr = 0$ are the upper limit up to the third harmonic and the lower limit for the higher harmonics ($n \geqslant 4$) of the heat flux variation. A conclusive physical interpretation of this behavior could not be found by the authors. With respect to practical applications, the most important finding is that most attention has to be devoted to the wall temperature variation due to the first harmonic of the heat flux. For this case, the ratio is remarkably greater than 1, varying from about 3·1 for a fluid of $Pr = 0{\cdot}007$ (sodium) at $Re \approx 60\,000$ to about 1·15 for a fluid of $Pr = 8$ (water) at same Reynolds number. It has to be kept in mind, however, that the ratio G_1/G_0 relates the maximum wall temperature variation above average to the average temperature drop due to the (averaged) constant heat flux. Thus, it cannot be concluded eo ipso from these figures for which fluids

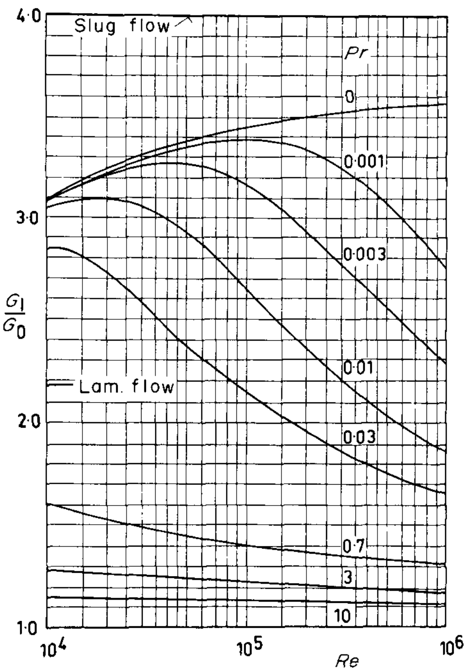

FIG. 14. Ratio of first harmonic of temperature function at the wall to average as a function of Reynolds number and Prandtl number.

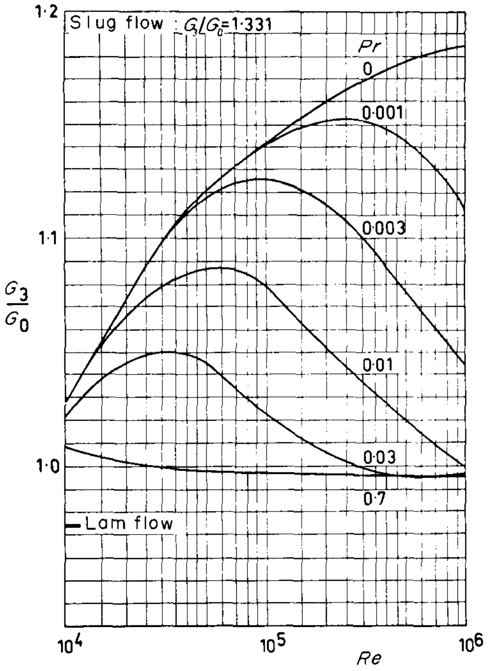

FIG. 15. Ratio of third harmonic of temperature function at the wall to average as a function of Reynolds number and Prandtl number.

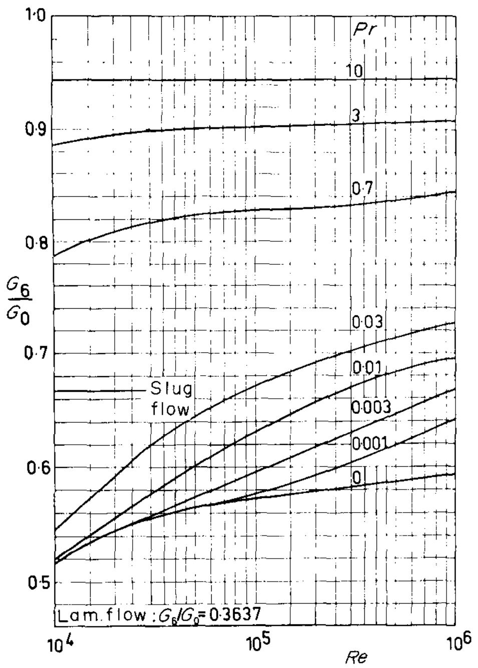

FIG. 16. Ratio of sixth harmonic of temperature function at the wall to average as a function of Reynolds number and Prandtl number.

the effect of circumferentially varying wall heat flux is more important. The resultant absolute wall temperature variation for a given heat flux amplitude may be of equal order of magnitude for a liquid-metal or water cooled heat transfer unit, since the values of the average temperature drop usually employed and the corresponding ratio G_1/G_0 behave contrarily.

Another interesting conclusion that may be drawn from Figs. 14–16 is related to the applicability of heat-transfer calculations assuming slug flow to estimate liquid-metal heat transfer. It is often believed that slug flow analysis yields the correct temperature fields for turbulent liquid-metal heat transfer at least for those combinations of Prandtl and Reynolds number at which the average Nusselt numbers agree with the slug flow result. Generally, this is not the case, since the ratios G_n/G_0 for slug flow do not have any points of intersection with the corresponding curves for turbulent liquid-metal heat transfer or do not intersect at the appropriate combination of *Re* and *Pr*. By slug flow analysis, the temperature variations are usually overestimated at the low harmonics and underestimated at the high harmonics.

The deviations of present results from those obtained by Reynolds [1] as well as Sutherland and Kays [36] are due to the different predictions used for velocity and eddy diffusivity distributions. This subject has been discussed in a previous section of this paper. It may be noted, however, that significant differences can be exclusively attributed to anisotropic turbulent energy diffusion which has been introduced in the present analysis. The effect of anisotropic eddy transport on first harmonic of the temperature function at the wall, G_1, is shown in Fig. 17. As expected, the increased turbulent transfer in the circumferential direction reduces the temperature function G_1. The reduction is the more pronounced the higher the contribution of turbulent transport to the total energy transport, i.e. it increases with both Reynolds and Prandtl numbers.

In Fig. 18, present theoretical results are compared with experimental data of Black and Sparrow [3, 4] for a tube with circumferentially varying boundary conditions. Temperature distributions at the inner tube surface have been taken from Black's thesis and used as input data to calculate corresponding wall heat flux and Nusselt number. The theoretical results of Sparrow and Lin [2] and Reynolds as taken from Black [3] are also plotted in Fig. 18. In general, all analyses predict Nusselt number variations which are more pronounced than those evaluated from the measurements. Present results seem to be closest to Black's data and, in view of the errors involved in the experiment as well as data reduction [14], the agreement is very satisfactory. The slightly lower level of present Nusselt number curves exhibits a difference in

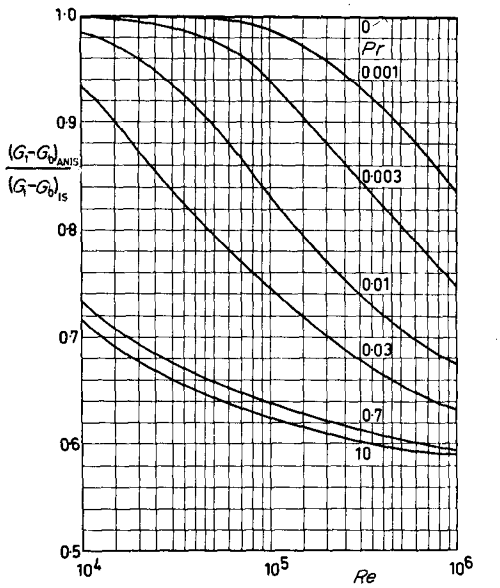

FIG. 17. Effect of anisotropy of turbulent energy transfer on first harmonic of temperature function at the wall.

average Nusselt numbers which previously has been shown in Fig. 12; calculated values are by about 4 per cent less than those measured by Black.

It seems rather surprising that Reynolds prediction deviates this much from both other predictions and measurements. From comparing with the Sparrow–Lin analysis, Black and Sparrow [3, 4] finally assumed that this could be due to the different turbulent transport model employed by Reynolds. It has been experienced by the authors, however, that the differences in eddy diffusivity distributions are by far too small to cause the rather large deviations of final results. The correct explanation may easily be found as soon as one recognizes that different problems are solved by Sparrow–Lin and Reynolds. Sparrow and Lin [2] considered the problem of prescribed circumferentially varying wall temperature (Case 2 of present paper) whereas Reynolds [1] developed a solution for the case of prescribed circumferentially varying wall heat flux. Obviously, Black and Sparrow introduced the measured circumferential temperature distributions into the Sparrow–Lin analysis to calculate the corresponding heat flux distribution and, by that, the Nusselt number variation. To compare with the Reynolds analysis, they took the heat flux distribution from Black's measurements to evaluate the corresponding temperature distribution (and Nusselt number). Even if identical velocity and eddy diffusivity distributions would have been used in both analyses, the deviations between the resultant temperature distributions as obtained by the latter procedure and that one used as boundary condition (Black's data) in the Sparrow–Lin analysis *must* be remarkably more pronounced than those between the corresponding wall heat fluxes. The reason becomes obvious by considering either Reynolds' or present results: A given heat flux

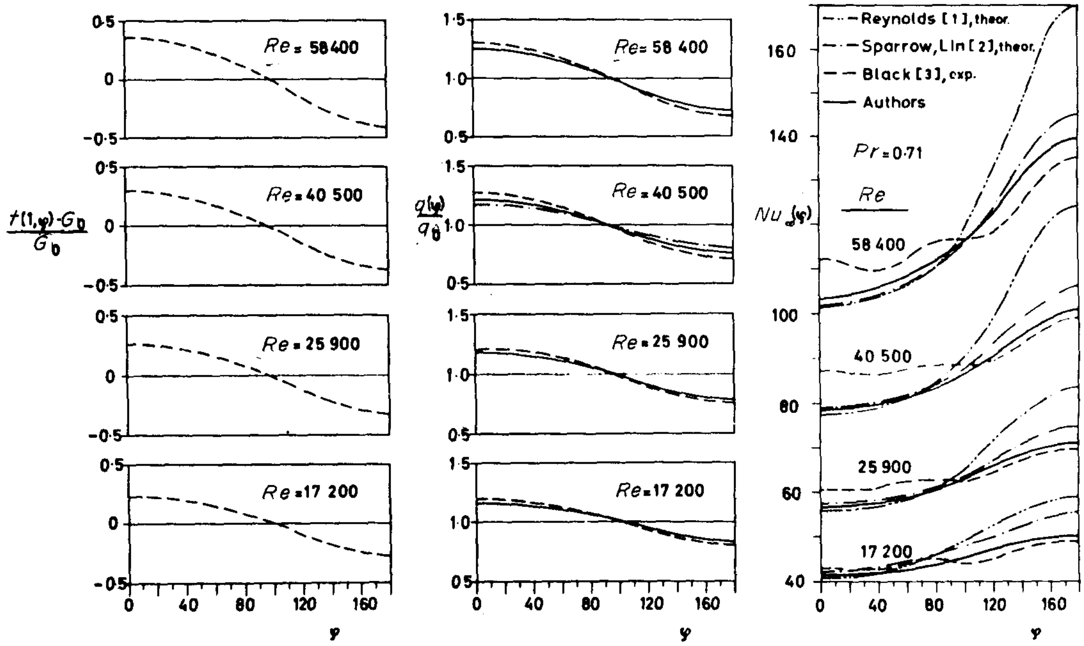

FIG. 18. Comparison of various theoretical results with experiment.

Table 1. Circumferential temperature functions $G_n = 2/Nu_{\infty 0}$

Pr	n	Re 10^4	3×10^4	10^5	3×10^5	10^6
0	0	0·3231	0·3034	0·2917	0·2848	0·2807
	1	1·0000	1·0000	1·0000	1·0000	1·0000
	2	0·5000	0·5000	0·5000	0·5000	0·5000
	3	0·3333	0·3333	0·3333	0·3333	0·3333
	4	0·2500	0·2500	0·2500	0·2500	0·2500
	5	0·2000	0·2000	0·2000	0·2000	0·2000
	6	0·1667	0·1667	0·1667	0·1667	0·1667
0·001	0	0·3230	0·3022	0·2834	0·2481	0·1751
	1	0·9989	0·9937	0·9561	0·8059	0·4853
	2	0·4995	0·4973	0·4817	0·4171	0·2699
	3	0·3331	0·3319	0·3232	0·2861	0·1950
	4	0·2498	0·2491	0·2436	0·2192	0·1553
	5	0·1999	0·1994	0·1956	0·1783	0·1301
	6	0·1666	0·1662	0·1635	0·1505	0·1125
0·003	0	0·3217	0·2958	0·2527	0·1817	0·1019
	1	0·9929	0·9613	0·8005	0·5042	0·2300
	2	0·4970	0·4837	0·4147	0·2792	0·1391
	3	0·3316	0·3243	0·2848	0·2013	0·1064
	4	0·2489	0·2442	0·2184	0·1600	0·08838
	5	0·1993	0·1960	0·1777	0·1339	0·07649
	6	0·1661	0·1637	0·1501	0·1157	0·06791
0·01	0	0·3125	0·2605	0·1730	0·09882	0·04638
	1	0·9499	0·7915	0·4567	0·2185	0·08667
	2	0·4787	0·4104	0·2562	0·1333	0·05694
	3	0·3215	0·2822	0·1866	0·1025	0·04596
	4	0·2425	0·2167	0·1495	0·08545	0·03969
	5	0·1948	0·1765	0·1258	0·07420	0·03543
	6	0·1629	0·1492	0·1092	0·06606	0·03227
0·03	0	0·2743	0·1830	0·09598	0·04775	0·02032
	1	0·7794	0·4705	0·2055	0·08883	0·03355
	2	0·4062	0·2638	0·1266	0·05857	0·02342
	3	0·2806	0·1923	0·09811	0·04738	0·01964
	4	0·2162	0·1543	0·08226	0·04099	0·01744
	5	0·1765	0·1300	0·07179	0·03664	0·01592
	6	0·1495	0·1130	0·06419	0·03342	0·01478
0·7	0	0·06967	0·02973	0·01147	0·004761	0·001774
	1	0·1116	0·04416	0·01610	0·006443	0·002317
	2	0·08165	0·03341	0·01252	0·005116	0·001879
	3	0·07029	0·02943	0·01118	0·004617	0·001714
	4	0·06352	0·02711	0·01040	0·004325	0·001616
	5	0·05869	0·02550	0·009861	0·004122	0·001548
	6	0·05494	0·02427	0·009452	0·003967	0·001496
3	0	0·03387	0·01344	0·004864	0·001950	0·0006977
	1	0·04398	0·01681	0·005940	0·002343	0·0008244
	2	0·03684	0·01429	0·005101	0·002032	0·0007221
	3	0·03407	0·01334	0·004787	0·001916	0·0006835
	4	0·03236	0·01279	0·004604	0·001847	0·0006608
	5	0·03110	0·01240	0·004477	0·001800	0·0006449
	6	0·03008	0·01209	0·004380	0·001763	0·0006327
10	0	0·02020	0·007778	0·002727	0·001084	0·0003774
	1	0·02328	0·008790	0·003048	0·001204	0·0004154
	2	0·02112	0·008031	0·002796	0·001111	0·0003847
	3	0·02028	0·007747	0·002702	0·001076	0·0003731
	4	0·01975	0·007579	0·002646	0·001055	0·0003663
	5	0·01935	0·007460	0·002608	0·001041	0·0003615
	6	0·01902	0·007366	0·002579	0·001030	0·0003579

Table 1. (cont.)

Pr	n	Re 10^4	3×10^4	10^5	3×10^5	10^6
30	0	0·01344	0·005109	0·001738	0·0007026	0·0002368
	1	0·01447	0·005442	0·001843	0·0007438	0·0002495
	2	0·01375	0·005188	0·001759	0·0007128	0·0002393
	3	0·01347	0·005093	0·001728	0·0007011	0·0002354
	4	0·01329	0·005037	0·001709	0·0006942	0·0002332
	5	0·01315	0·004997	0·001697	0·0006894	0·0002316
	6	0·01304	0·004965	0·001687	0·0006858	0·0002304
100	0	0·009098	0·003450	0·001069	0·0004710	0·0001449
	1	0·009408	0·003541	0·001097	0·0004844	0·0001486
	2	0·009191	0·003465	0·001072	0·0004751	0·0001455
	3	0·009105	0·003436	0·001063	0·0004716	0·0001444
	4	0·009051	0·003419	0·001057	0·0004695	0·0001437
	5	0·009009	0·003407	0·001053	0·0004681	0·0001432
	6	0·008973	0·003397	0·001050	0·0004670	0·0001428

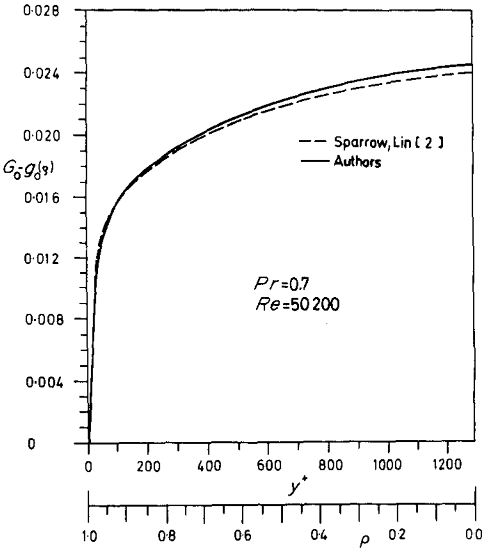

FIG. 19. Comparison of present result for fully-developed radial temperature profile at constant wall heat flux with that of Sparrow–Lin analysis.

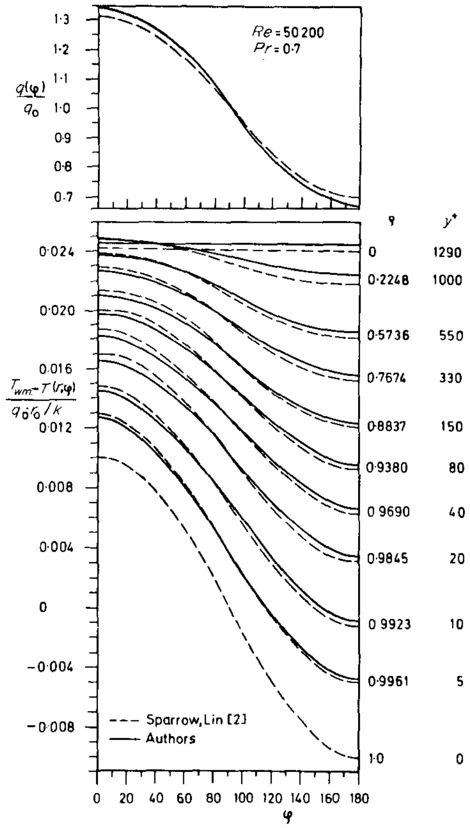

FIG. 20. Comparison of present results for prescribed wall temperature variation with those of Sparrow and Lin [2].

variation of first harmonic results in a greater corresponding temperature variation. Thus, small differences in heat flux distributions result in remarkably greater differences of the corresponding temperature distributions as well, while just the opposite is true for temperature variations with respect to corresponding heat flux variations.

In Figs. 19 and 20, present results for prescribed wall temperature are compared to those of Sparrow and Lin [2]. The differences in the solutions for the radial temperature profile at constant wall temperature are due to the slightly different radial distributions used for turbulent velocity and thermal eddy diffusivity in the radial direction. Figure 20 mainly exhibits the effect of anisotropy of turbulent energy transport on the dimensionless temperature field within the fluid,

$$\frac{T_{wm}-T(r,\varphi)}{q_0 \cdot r_0/k} = G_0 - g_0 + g_1(\rho,\varphi),$$

and the corresponding wall heat flux when a circumferentially varying wall temperature is prescribed.

Acknowledgements—The authors would like to express their appreciation to Mrs. Waltraud Jahnke for typing the manuscript.

Thanks are also due to the Technische Universität Berlin for granting a fellowship to the first author (D. G.) and to the German Research Foundation for its financial support of the work contributed by the last author (H. R.). Without this generous financial support the work reported herein could not have been done.

REFERENCES

1. W. C. Reynolds, Turbulent heat transfer in a circular tube with variable circumferential heat flux, *Int. J. Heat Mass Transfer* **6**, 445–454 (1963).
2. E. M. Sparrow and S. H. Lin, Turbulent heat transfer in a tube with circumferentially-varying temperature or heat flux, *Int. J. Heat Mass Transfer* **6**, 866–867 (1963).
3. A. W. Black, The effect of circumferentially varying boundary conditions on turbulent heat transfer in a tube, Ph. D. thesis, Dept. of Mechanical Engineering, Univ. of Minnesota, Minneapolis, Minn. (1966).
4. A. W. Black and E. M. Sparrow, Experiments on turbulent heat transfer in a tube with circumferentially varying thermal boundary conditions, *J. Heat Transfer* **89**, 258–268 (1967).
5. V. P. Bobkov, M. Kh. Ibragimov and V. I. Subbotin, Calculating the coefficient of turbulent heat transfer for a liquid flowing in a tube, *Sov. At. Energy* **24**, 545–550 (1968).
6. H. Ramm and K. Johannsen, Radial and tangential turbulent diffusivities for heat and momentum transfer in liquid metals, [Int. Seminar on "Heat Transfer in Liquid Metals", Trogir, Yugoslavia (1971)] *Progress in Heat and Mass Transfer*, Vol. 7, pp. 45–58. Pergamon Press, Oxford (1973).
7. H. Ramm and K. Johannsen, Hydrodynamics and heat transfer in regular arrays of circular tubes, Int. Seminar on "Recent Developments in Heat Exchangers", Trogir, Yugoslavia (1972).
8. N. I. Buleev, Theoretical model of the mechanism of turbulent exchange in fluid flow, Report AERE-Trans 957. Engl. translation from: Teploperedacha, USSR Academy of Science, Moscow, pp. 64–98 (1962).
9. N. I. Buleev, Theoretical model for turbulent transfer in three-dimensional fluid flow, 3rd UN Intern. Conf. Peaceful Uses At. Energy, Geneva, Paper No. 329 (1964).
10. J. Laufer, The structure of turbulence in fully developed pipe flow, NACA Report No. 1174 (1954).
11. C. J. Lawn and C. J. Elliott, Fully developed turbulent flow through concentric annuli, Report RD/B/N 1878 (1971).
12. A. Quarmby, Calculations of the effect of tangential eddy diffusivity on a non-symmetric turbulent diffusion in a plain tube, *Int. J. Heat Mass Transfer* **15**, 866–870 (1972).
13. H. Ramm and K. Johannsen, Turbulent transport properties for thermal design of LMFBR Cores, *Trans. Am. Nucl. Soc.* **15**, 857–858 (1972).
14. A. C. Rapier, Forced convection heat transfer in a circular tube with on-uniform heat flux around the circumference, *Int. J. Heat Mass Transfer* **15**, 527–538 (1972).
15. R. Jenkins, Variation of the eddy conductivity with Prandtl modulus and its use in prediction of turbulent heat transfer coefficients, Heat Transfer and Fluid Mechanics Institute (preprints), Stanford University Press, Stanford, California (1951).
16. C. A. Sleicher, Jr., Experimental velocity and temperature profiles for air in turbulent pipe flow, *Trans. Am. Soc. Mech. Engrs* **80**, 693–704 (1958).
17. B. Kjellström, Transport processes in turbulent channel flow, Report AE-RL-1344 (1972).
18. J. R. Tyldesley and R. S. Silver, The prediction of the transport properties of a turbulent fluid, *Int. J. Heat Mass Transfer* **11**, 1325–1340 (1968).
19. H. Fuchs and S. Faesch, Measurement of eddy conductivity in sodium [Int. Seminar on "Heat Transfer in Liquid Metals", Trogir, Yugoslavia (1971)] *Progress in Heat and Mass Transfer*, Vol. 7, pp. 39–43. Pergamon Press, Oxford (1973).
20. N. Sheriff and D. J. O'Kane, Sodium eddy diffusivity of heat measurements in a circular duct [Int. Seminar on "Heat Transfer in Liquid Metals", Trogir, Yugoslavia (1971)] in *Progress in Heat and Mass Transfer*, Vol. 7, pp. 25–38. Pergamon Press, Oxford (1973).
21. H. Fuchs, Wärmeübergang an strömendes Natrium. EIR-Report No. 241 (1973).
22. V. I. Subbotin; M. Kh. Ibragimov and E. V. Nomofilov, Generalized equation for turbulent-heat-transfer coefficient with fluid flow, *High Temperature* **3**, 380–384 (1965).
23. W. Hufschmidt, E. Burck and W. Riebold, Die Bestimmung örtlicher und mittlerer Wärmeübergangszahlen in Rohren bei hohen Wärmestromdichten, *Int. J. Heat Mass Transfer* **9**, 539–565 (1966).
24. R. W. Allen and E. R. G. Eckert, Friction and heat-transfer measurements to turbulent pipe flow of water ($Pr = 7$ and 8) at uniform wall heat flux, *J. Heat Transfer* **86**, 301–310 (1964).
25. B. S. Petukhov and V. N. Popov, Theoretical calculation of heat exchange and frictional resistance in turbulent flow in tubes of an incompressible fluid with variable physical properties, *High Temperature* **1**, 69–83 (1963).
26. A. Quarmby and R. Quirk, Measurements of the radial and tangential eddy diffusivities of heat and mass in turbulent flow in a plain tube, *Int. J. Heat Mass Transfer* **15**, 2309–2327 (1972).
27. K. Johannsen and H. Ramm, Note on tangential eddy diffusivity in a circular tube, *Int. J. Heat Mass Transfer* **16**, 1803–1805 (1973).
28. H. Ramm and K. Johannsen, Prediction of local and

integral turbulent transport properties for liquid-metal heat transfer in equilateral triangular rod arrays, *J. Heat Transfer*, In press.
29. R. L. Webb, A critical evaluation of analytical solutions and Reynolds analogy equations for turbulent heat and mass transfer in smooth tubes, *Wärme- und Stoffübertragung* **4**, 197–204 (1971).
30. W. M. Kays and E. Y. Leung, Heat transfer in annular passages—hydrodynamically developed turbulent flow with arbitrarily prescribed heat flux, *Int. J. Heat Mass Transfer* **6**, 537–557 (1963).
31. E. M. Sparrow, T. M. Hallman and R. Siegel, Turbulent heat transfer in the thermal entrance region of pipe with uniform heat flux, *Appl. Scient. Res.* **A7**, 37–52 (1958).
32. A. Eagle and R. M. Ferguson, The coefficients of heat transfer from tube to water, *Proc. Inst. Mech. Engrs* **2**, 985 (1930).
33. R. C. Hastrup, Heat transfer and pressure drop in an artificially roughed tube at various Prandtl numbers, M. S. Thesis, Calif. Inst. of Techn. (1958).
34. J. P. Hartnett, Experimental determination of the thermal entrance length for the flow of water and of oil in circular pipes, *Trans. Am. Soc. Mech. Engrs* **77**, 1211–1220 (1955).
35. J. A. Malina and E. M. Sparrow, Variable-property, constant-property, and entrance-region heat transfer results for turbulent flow of water and oil in a circular tube, *Chem. Engng Sci.* **19**, 953–962 (1964).
36. W. A. Sutherland and W. M. Kays, Heat transfer in an annulus with variable circumferential heat flux, *Int. J. Heat Mass Transfer* **7**, 1187–1194 (1964).
37. H. Ramm, Theoretisches Modell zur Beschreibung des Impuls- und Energietransports in turbulenter Kanalströmung, TUBIK Report No. 31 (1974).

TRANSFERT THERMIQUE TURBULENT DANS UN TUBE CIRCULAIRE AVEC DES CONDITIONS AUX LIMITES VARIANT SUR LA CIRCONFERENCE

Résumé—Cette analyse détermine les caractéristiques d'un écoulement turbulent dans un tube circulaire avec des conditions aux limites de première et de seconde espèce variables sur la circonférence.

On considère un écoulement dynamiquement et thermiquement établi. Contrairement aux études antérieures, on prend en compte l'anisotropie du transport d'énergie turbulente en s'appuyant sur les résultats théoriques de Ramm et Johansen qui sont en accord satisfaisant avec les récents résultats expérimentaux. Les résultats sur le transfert thermique avec des conditions aux limites constantes ou variables sont présentés pour un large domaine de nombre de Reynolds ($10^4 \leqslant Re \leqslant 10^6$) et de nombre de Prandtl ($0 \leqslant Pr \leqslant 100$) et ils sont comparés aux relations empiriques.

TURBULENTE WÄRMEÜBERTRAGUNG IN EINEM KREISROHR MIT UMFANGSVARIABLEN THERMISCHEN RANDBEDINGUNGEN

Zusammenfassung—Die Wärmeübertragungseigenschaften einer turbulenten Strömung in einem Kreisrohr wurden für den Fall umfangsvariabler Randbedingungen erster und zweiter Art theoretisch untersucht. Die Analyse setzt voll ausgebildete Geschwindigkeits- und Temperaturfelder voraus. Im Gegensatz zu früheren Untersuchungen des gleichen Problems wurde die Anisotropie des turbulenten Energietransports berücksichtigt. Die benutzten Verteilungen für die richtungsabhängigen turbulenten Austauschgrößen wurden nach einem von Ramm und Johannsen entwickelten Verfahren berechnet; die befriedigende Übereinstimmung der theoretisch ermittelten Verteilungen mit neueren Meßergebnissen wird nachgewiesen. Ergebnisse für den Wärmeübergang bei konstanten und umfangsvariablen Randbedingungen werden für einen weiten Bereich der Reynolds-Zahl ($10^4 \leqslant Re \leqslant 10^6$) und Prandtl-Zahl ($0 \leqslant Pr \leqslant 100$) angegeben und mit Meßergebnissen verglichen.

ТУРБУЛЕНТНЫЙ ТЕПЛООБМЕН В КРУГЛОЙ ТРУБЕ ПРИ ТЕПЛОВЫХ ГРАНИЧНЫХ УСЛОВИЯХ, ИЗМЕНЯЮЩИХСЯ ПО ОКРУЖНОСТИ

Аннотация — Определяются характеристики теплообмена в турбулентном потоке в круглой трубе при граничных условиях первого и второго рода, изменяющихся по окружности. Рассматривается полностью развитое течение и теплообмен. В отличие от предыдущих исследований данной проблемы, в настоящей работе учитывается анизотропия турбулентного переноса энергии на основе теоретических результатов Рамма и Джохансена по турбулентной температуропроводности в различных направлениях. Показано, что эти результаты хорошо согласуются с недавно полученными экспериментальными данными. Результаты по теплообмену при постоянных и переменных граничных условиях представлены в широком диапазоне значений чисел Рейнольдса ($10^4 \leqslant Re \leqslant 10^6$) и Прандтля ($0 \leqslant Pr \leqslant 100$) и проведено сравнение с эмпирическими данными.